PAPER • OPEN ACCESS

Phase diagrams of the diode effect in superconducting heterostructures

To cite this article: T Karabassov *et al* 2024 *Phys. Scr.* **99** 015010

Physica Scripta

PAPER

Phase diagrams of the diode effect in superconducting heterostructures

T Karabassov[1], I V Bobkova[1,2], V M Silkin[3,4,5], B G Lvov[1], A A Golubov[6] and A S Vasenko[1,7]

[1] HSE University, 101000 Moscow, Russia
[2] Moscow Institute of Physics and Technology, Dolgoprudny, Moscow 141700, Russia
[3] Donostia International Physics Center (DIPC), San Sebastián/Donostia, 20018 Basque Country, Spain
[4] Departamento de Física de Materiales, Facultad de Ciencias Químicas, UPV/EHU, 20080 San Sebastián, Basque Country, Spain
[5] IKERBASQUE, Basque Foundation for Science, 48011 Bilbao, Spain
[6] Faculty of Science and Technology and MESA+ Institute for Nanotechnology, University of Twente, 7500 AE Enschede, The Netherlands
[7] I.E. Tamm Department of Theoretical Physics, P.N. Lebedev Physical Institute, Russian Academy of Sciences, 119991 Moscow, Russia

E-mail: a.golubov@utwente.nl

Keywords: Superconducting diode effect, proximity effect, superconductor/ferromagnet junctions, topological insulator, superconducting hybrid structures, spin-orbit interaction

OPEN ACCESS

RECEIVED
22 September 2023

REVISED
6 November 2023

ACCEPTED FOR PUBLICATION
7 December 2023

PUBLISHED
19 December 2023

Abstract

At present the superconducting diode effect (SDE) attracts a lot of attention due to new possibilities in the superconducting electronics. One of the possible realizations of the SDE is the implementation in superconducting hybrid structures. In this case the SDE is achieved by means of the proximity effect. However, the optimal conditions for the SDE quality factor in hybrid devices remain unclear. In this study we consider the Superconductor/Ferromagnet/Topological insulator (S/F/TI) hybrid device and investigate the diode quality factor at different parameters of the hybrid structure. Consequently, we reveal important parameters that have crucial impact on the magnitude of the SDE quality factor.

1. Introduction

The superconducting (or supercurrent) diode effect (SDE) is the superconducting analog of the semiconducting diode effect in $p-n$ junctions. While in normal systems the diode effect corresponds to the conduction of the normal current in the only one direction, the superconducting diode effect involves the nonreciprocity of the supercurrent [1]. The discovery of such effect brings many potential applications in low-power logic circuits as quantum computing and spin-based electronics [2, 3].

Various systems that can behave as superconducting diodes have been recently theoretically proposed [4–13] and experimentally discovered [14–23]. The superconducting diode effect can be realized in two-dimensional (2D) superconducting systems if both inversion and time-reversal symmetries are broken[1]. One of the most promising SDE devices are Josephson diodes, where weak link plays the key role in achieving the current nonreciprocity [24–39]. As it has been shown recently the SDE in Josephson junctions may be due to the only inversion symmetry breaking and do not require the time-reversal symmetry breaking [29]. It can be implemented in the weak links with voltage dependent Rashba spin–orbit coupling (SOC) or electric polarization, which leads to $I_c(V) \neq I_c(-V)$, where I_c is the Josephson critical current.

The 'conventional' SDE devices require both inversion and time-reversal symmetry breaking in 2D superconducting films [1]. The inversion symmetry can be broken by introducing the spin–orbit coupling. Experimentally it can be achieved in hybrid structures by proximity to a three-dimensional topological insulator (TI), in superconductors with Rashba spin–orbit coupling (like in polar $SrTiO_3$ films[40], few-layer $MoTe_2$ in the T_d phase or MoS_2 [6, 41, 42], and twisted bilayer graphene[43, 44]), or, in some cases, by the asymmetry of the device geometry. On the other hand, the time-reversal symmetry can be broken by the in-plane magnetic field, or alternatively in hybrid structures by proximity to a ferromagnetic insulator with the in-plane exchange field. Such conditions can lead to $I_c^+ \neq I_c^-$ (Here I_c^+ and I_c^- are the critical currents in the opposite directions).

The breaking of time-reversal and inversion symmetries in 2D superconductors allows for a formation of the helical superconducting phase [45–50], with the order parameter modulated in the direction transverse to the magnetic (or exchange) in-plane field: $\Delta(\boldsymbol{r}) = \Delta \exp(i\boldsymbol{q_0}\boldsymbol{r})$. Such superconducting state with finite $\boldsymbol{q_0}$ resembles the FFLO state [51–54].

The coexistence of exchange field, superconductivity and SOC is rare and underexplored with respect to magnetoelectric effects [55]. At the same time bringing all ingredients together can be easily achieved in hybrid devices based on a combination of conventional materials: superconductors (S), three-dimensional topological insulators (TI) and ferromagnet (F). Hybrid superconducting diode can be realized as a F/S/TI/S/F Josephson junction (Josephson SDE) [39], or an S/F hybrid on top of a TI (SDE realized by proximity effect) [56, 57]. The latter scenario is examined in this article, focusing on TI as the material of choice due to its conductive surface state featuring full spin-momentum locking caused by a particularly strong SOC [58–61]. It has been noted in previous studies that even if the exchange field and superconducting order parameter are separate spatially, a finite-momentum superconducting helical state occurs due to the proximity effect. This state is characterized by spontaneously generated currents running parallel to the S/F interface, with an uneven distribution over the bilayer resulting in a net current equal to zero [57]. The necessary condition for this hybrid state to arise is a Zeeman field component perpendicular to the S/F interface. Such superconducting state is nonreciprocal and can be used as a superconducting diode. Namely if a current parrallel to the S/F interface flows in such a structure, in one direction it is a supercurrent, whereas in other direction it can be a dissipative current.

The nonreciprocity of the critical current can be quantified by the superconducting diode quality factor,

$$\eta = \frac{I_c^+ - I_c^-}{I_c^+ + I_c^-}, \tag{1}$$

where the $I_c^{\pm}$ are external positive and negative currents parallel to the S/FI interface. We have already shown that η is finite in the considered system [57]. However, the optimal conditions for the SDE quality factor remain unclear. In this paper we investigate the diode quality factor of the hybrid structure, studying the phase diagrams of the superconducting diode effect for various parameters of the S/F/TI hybrid structure which influence the superconducting diode effect. We employ the microscopic quasiclassical approach and calculate the diode quality factor within the Usadel equations. This study can be useful for the experimental fabrication of the superconducting diode with sufficiently good efficiency for applications in superconducting electronics.

The structure of the article is as follows: In section 2, we present the mathematical model of the proximity effect in the hybrid structure under consideration. In section 3, we apply this theory to determine the phase diagrams of the superconducting diode effect for different parameters of the hybrid structure. Finally, in section 4, we provide a summary of the essential findings of the study.

2. Model

In the present part we introduce the system under consideration depicted in figure 1. The hybrid system is represented by a thin layer superconductor (S) in contact with a ferromagnetic insulator region (F) which are placed on top of the topological insulator. In this situation we have strong spin–orbit coupling from the conductive surface of the TI that leads to the pronounced spin-momentum locking effect. Such two-dimensional system can be described in real space in the following way:

$$H = H_0 + H_F + H_S, \tag{2}$$

where

$$H_0 = \int d^2r \Psi^\dagger(\boldsymbol{r})[-i\alpha(\boldsymbol{\nabla_r} \times \hat{z})\boldsymbol{\sigma} - \mu + V(\boldsymbol{r})]\Psi(\boldsymbol{r}), \tag{3}$$

$$H_S = \Delta(\boldsymbol{r})\Psi_\uparrow^\dagger(\boldsymbol{r})\Psi_\downarrow^\dagger(\boldsymbol{r}) + \Delta^*(\boldsymbol{r})\Psi_\downarrow(\boldsymbol{r})\Psi_\uparrow(\boldsymbol{r}), \tag{4}$$

$$H_F = -\int d^2r \Psi^\dagger(\boldsymbol{r})[\boldsymbol{h}\boldsymbol{\sigma}]\Psi(\boldsymbol{r}). \tag{5}$$

In the Hamiltonian above $\Psi(\boldsymbol{r})$ and $\Psi^\dagger(\boldsymbol{r})$ correspond to the annihilation and creation operators of an electronic state at the TI surface. $\hat{z}$ is the unit vector along the direction perpendicular to the TI surface, μ is the chemical potential, α is the Fermi velocity, $\boldsymbol{h}$ is the exchange field that exists only at $x < 0$ and $\boldsymbol{h} = (h_x, h_y, 0)$, finally $\boldsymbol{\sigma}$ is the Pauli matrix vector. The superconducting pairing potential Δ exists only at $x > 0$, thereby dividing the TI surface into effectively two parts: one that possesses $h \neq 0$ at $x < 0$, called 'ferromagnetic', and the other at $x > 0$ with $\Delta \neq 0$, referred to as 'superconducting'. The energy potential $V(\boldsymbol{r})$ contains an impurity scattering potential $V_{imp} = \sum_{\boldsymbol{r_i}} V_i \delta(\boldsymbol{r} - \boldsymbol{r_i})$ represented by a Gaussian form $\langle V(\boldsymbol{r})V(\boldsymbol{r'})\rangle = (1/\pi\nu\tau)\delta(\boldsymbol{r} - \boldsymbol{r'})$ with $\nu = \mu/(2\pi\alpha^2)$. In this work we assume that $h_y = 0$ and consider the nonzero component normal to the S/F interface $h_x = h$. In fact, it can be demonstrated that finite h_y does not influence the observables in the model under consideration and produces only a characteristic phase shift, which is irrelevant in our hybrid structure [56, 62]. Such phase

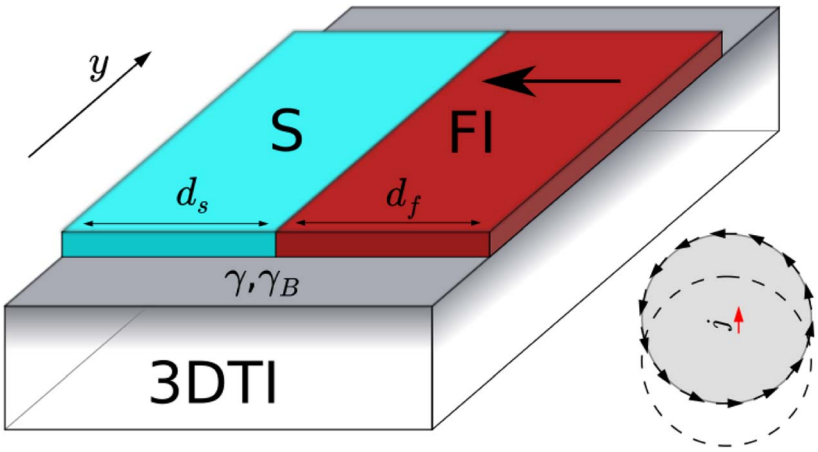

Figure 1. (a) The S/F (Ferromagnetic insulator) bilayer deposited on the surface of the 3D TI. Right bottom corner: Fermi-contour of the TI surface states with the spin-momentum locking property and the illustration of the magnetolectric effect.

shift would be important in the Josephson junction hybrid structure, since it can control the phase difference between the two superconducting regions [62].

It has been shown previously that the SOC term in the Hamiltonian (2) leads to the spinless structure of the Green's functions [62, 63]. This situation takes place because of the full spin-momentum locking effect, i. e. the direction of the quasiparticle momentum is locked with the direction of its spin at the right angle. That is why the spin is not a good quantum number and the quasiparticle states can be considered as spinless fermiones in the model.

We formulate the model in the formalism of the Usadel equations. In the conductors with high density of impurities the mean free path of electrons l is much smaller than all the other length scales. In this situation it is appropriate to assume that the Green's functions of the system are isotropic in the first approximation. The description of the quasiclassical Green's functions behavior in this limit corresponds to the Usadel equation. It has been shown that the surface states of the TI in the presence of an in-plane exchange field obey the following Usadel equation (F part ($x < 0$)) [62, 63]:

$$D_f \hat{\nabla}(\hat{g}_f \hat{\nabla}\hat{g}_f) = [\omega_n \tau_z, \hat{g}_f]. \tag{6}$$

Here we have the following notation: ω_n is the Matsubara frequency, D_f is the diffusion coefficient in the F part and τ_z is the Pauli matrix in the Nambu space. The exchange field $\boldsymbol{h}$ enters the Usadel equation as an effective vector potential through the covariant derivative $\hat{\nabla}X = \nabla X + i(h_x\hat{e}_y - h_y\hat{e}_x)[\tau_z, \hat{g}]/\alpha$. The Usadel equation in the S part reads ($x > 0$),

$$D_s \nabla(\hat{g}_s \nabla\hat{g}_s) = [\omega_n \tau_z + i\hat{\Delta}, \hat{g}_s], \tag{7}$$

$$\hat{\Delta} = i\begin{pmatrix} 0 & \Delta \\ \Delta^* & 0 \end{pmatrix}. \tag{8}$$

Here D_s is the diffusion coefficient in the S part, Δ is the superconducting gap that satisfies the self-consistency equation and $\hat{g}_s$ is the S region Green's function matrix. The geometry in the model is assumed to be finite along the x-axis and infinite along the y-axis. In order to consider a finite momentum Cooper pair state, we assume the superconducting pair potential of the following form

$$\Delta(\boldsymbol{r}) = \Delta(x)e^{iqy}, \tag{9}$$

where q is the momentum of the Cooper pair. The Usadel equations should be supplemented with the quasiclassical boundary conditions[64]:

$$\gamma\xi_f \hat{g}_f \hat{\nabla}\hat{g}_f = \xi_s \hat{g}_s \nabla\hat{g}_s, \tag{10}$$

$$\gamma_B \xi_f \hat{g}_f \hat{\nabla}\hat{g}_f = [\hat{g}_f, \hat{g}_s]. \tag{11}$$

Here parameters $\gamma_B = R_B\sigma_f/\xi_f$, $\gamma = \xi_s\sigma_f/\xi_f\sigma_s$ where $\sigma_{s(f)}$ is the conductivity of the S (F) part. The characteristic length $\xi_{s(f)} = \sqrt{D_{s(f)}/2\pi T_{cs}}$, where T_{cs} is the transition temperature of the S region in the absence of adjacent ferromagnetic part F. Parameter γ controls the slope of the Green's functions at the interface, whereas γ_B controls the mismatch between the functions at the interface. While for identical materials $\gamma = 1$, in general this parameter may have arbitrary value. γ_B is the parameter that determines the transparency of the S/F interface [64–66]. While for an ideal fully transparent interface $\gamma_B = 0$, in general case one may expect finite value of γ_B.

Both of the parameters are responsible for the description of the proximity effect in the diffusive systems. In this work we will study the dependence of the diode efficiency on the values of γ and γ_B in order to find optimal conditions for the best diode efficiency.

θ - parametrization of the Green's functions is used in the calculations for its convenience [67], i. e. $\hat{g}_{11} = \cos\theta$ and $\hat{g}_{12} = \sin\theta$. Such parametrization automatically satisfies the normalization condition $\hat{g}\hat{g} = 1$. We then substitute the above expression into the equation (7) and obtain the equation in the S part of the TI:

$$\xi_s^2\left[\partial_x^2\theta_s - \frac{q^2}{2}\sin 2\theta_s\right] = \frac{1}{\pi T_{cs}}[\omega_n \sin\theta_s - \Delta(x)\cos\theta_s],$$

We achieve self-consistency in the solution of the problem by solving the equation for the s-wave pair potential $\Delta(x)$

$$\Delta(x)\ln\frac{T_{cs}}{T} = \pi T\sum_{\omega_n}\left(\frac{\Delta(x)}{|\omega_n|} - 2\sin\theta_s\right). \tag{12}$$

Similarly the Usadel equation in θ - parametrization in the F part :

$$\xi_f^2\left[\partial_x^2\theta_f - \frac{q_m^2}{2}\sin 2\theta_f\right] = \frac{\omega_n}{\pi T_{cs}}\sin\theta_f, \tag{13}$$

where $q_m = q + 2h/\alpha$.

Turning to the boundary conditions, at the free edges of the hybrid structure we require zero current flow through the boundaries,

$$\frac{\partial\theta_f}{\partial x}\bigg|_{x=-d_f} = 0, \quad \frac{\partial\theta_s}{\partial x}\bigg|_{x=d_s} = 0. \tag{14}$$

At the interface ($x = 0$) the following conditions should be satisfied

$$\frac{\gamma_B}{\gamma}\frac{\partial\theta_s}{\partial x}\bigg|_{x=0} = \sin(\theta_s - \theta_f), \tag{15}$$

$$\gamma_B\frac{\partial\theta_f}{\partial x}\bigg|_{x=0} = \sin(\theta_s - \theta_f). \tag{16}$$

The supercurrent density is calculated with the help of the following expression

$$\mathbf{J}_{s(f)} = \frac{-i\pi\sigma_{s(f)}}{4e}T\sum_{\omega_n} Tr[\tau_z\hat{g}_{s(f)}\hat{\nabla}\hat{g}_{s(f)}]. \tag{17}$$

This supercurrent relation (17) is different from the conventional current formula, since it contains the covariant derivative $\hat{\nabla}$ that takes into account the spin-momentum locking effect. Using the parameterized Green's functions the supercurrent densities in the F and S parts can be written as

$$j_y^f(x) = -\frac{\pi\sigma_f}{2e}\left[q + \frac{2h}{\alpha}\right]T\sum_{\omega_n}\sin^2\theta_f, \tag{18}$$

$$j_y^s(x) = -\frac{\pi\sigma_s q}{2e}T\sum_{\omega_n}\sin^2\theta_s. \tag{19}$$

In order to compute the total superconducting current we perform integration over the widths of the F and S parts along the x axis. In what follows we present the phase diagrams of the quality factor defined in equation (1). In order to compute η we find the critical supercurrents $I_c^{+(-)}$ by calculating the total supercurrent versus Cooper pair momentum q and finding the maximum and minimum values of $I(q)$.

3. Results

In the present section we introduce the results of the superconducting current calculations. Here we use $\xi_f = \xi_s$ and dimensionless exchange field $H = \xi h/\alpha$.

In figure 2 the dependence of the quality factor η as a function of temperature T and exchange field H is demonstrated. The exchange field in the considered system can be changed by rotating the magnetization of the adjacent F part. Since the magnetization component along the interface does not introduce any quantitative effect on the observable quantities, the projection onto the x axis h_x (component normal to the interface) of the in-plane magnetization $\boldsymbol{h} = h_0(\cos\phi,\ \sin\phi,\ 0)$ (ϕ is the angle between $\boldsymbol{h}$ and x axis) can be varied by rotating the magnetization angle ϕ. From figure 2 we can notice several important observations. First, we can see that η

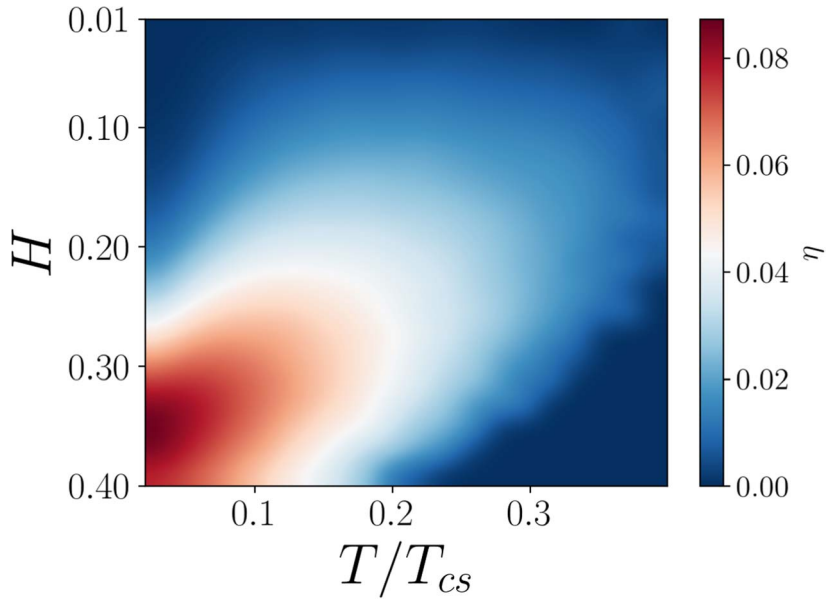

Figure 2. $H-T$ phase diagram of the diode efficiency η. The parameters of the calculation: $\gamma=0.5, \gamma_B=0.3, d_s=1.2\xi, d_f=\xi$.

has the largest value at a low temperature. For given parameters the maximum value of η corresponds to $H\approx 0.35$. From the figure we can observe that the quality factor decreases as the temperature increased, which is in agreement with the previous studies in other systems [4, 5, 8, 39]. The boundary that corresponds to the vanishing of η determines the critical exchange field H_c that destroys the superconducting state in the system. It is unlikely that this boundary may correspond to the $\eta=0$ in the superconducting state. This can be confirmed by simple analytical calculations in the vicinity of the critical temperature. For instance, in the limit of $d_f\ll d_s$ and $Hd_f/\xi\ll 1$ the quality factor can be written as [57]

$$\eta\approx\frac{1}{2}\frac{\sqrt{7\zeta(2)\zeta(3)}}{(T/T_{cs})^{5/2}}\frac{Hd_f}{d_s}\approx 1.86\frac{1}{(T/T_{cs})^{5/2}}\frac{Hd_f}{d_s}. \tag{20}$$

Here we can see that the quality factor is governed by the parameters of the F part, d_f and H. From this expression we can see that as long as the exchange field H and the width d_f are finite the quality factor is distinct from zero. These parameters are non zero in our case, hence the SDE should be present even at the vicinity of the critical temperature T_c. For this reason it is safe to note that this boundary corresponds to the critical field H_c.

It is important to note that in the our relatively simplified hybrid system it is impossible to observe the sign change of the SDE. i. e. when $\eta<0$ [4, 8]. We consider the system in which the spin structure of the correlations is projected onto a single helical band. In this case we do not take into account the competition between the bands with the opposite helical states, since the second band is not considered.

In figure 3 we plot the diode quality factor as a function of the S and F parts widths, which are d_s and d_f respectively. This plot has important features that characterize the considered system. From the diagram we can recognize the sharp transition from $\eta=0$ to a nonzero value. This rapid change corresponds to the transition between normal and superconducting state and can be characterized by the critical width of the S part d_s^{crit}. It can be seen from the figure that there is an optimal value of d_s and d_f to reach the highest quality factor η. For larger d_s and d_f the quality factor will gradually decline since the characteristic lengths of the superconducting correlations in the S and F parts become smaller than the geometrical sizes of the hybrid structure.

Another important aspect of this study is to investigate the parameters that control the proximity effect. In figure 4 $\gamma-\gamma_B$ diagram for η is illustrated. Interestingly, one can notice that there is an optimal nonzero value of the interface transparency parameter γ_B, i. e. having a perfect transparency does not result in a better diode efficiency. This can be explained by the following argument. When the transparency of the interface is low ($\gamma_B>1$) the proximity effect is strongly suppressed, the mutual coupling between S and F parts of the structure becomes weaker. Thus, the SDE reduces as γ_B keeps increasing. On the other hand, when $\gamma_B<1$ there can be one of the two cases depending on the value of γ. In the case when $\gamma>0.5$ the inverse proximity effect becomes too strong and the superconducting state in the S part is suppressed. Hence, this results in the vanishing of the SDE. When $\gamma<0.5$ the superconductivity does not vanish, but the diode effect is small at $\gamma_B\approx 0$ and reaches its maximum value at finite γ_B. From this result we conclude that for the highest η it is optimal to have a finite transparency parameter across the S/F interface.

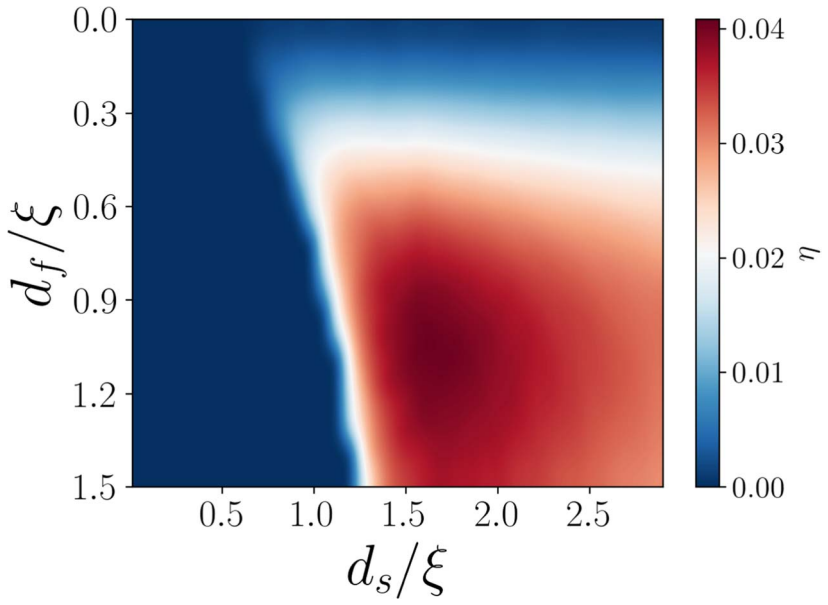

Figure 3. Phase diagram of the diode efficiency η plotted on the axes $d_s - d_f$. The parameters of the calculation: $\gamma = 0.5$, $\gamma_B = 0.3$, $T = 0.25T_{cs}$, $H = 0.3$.

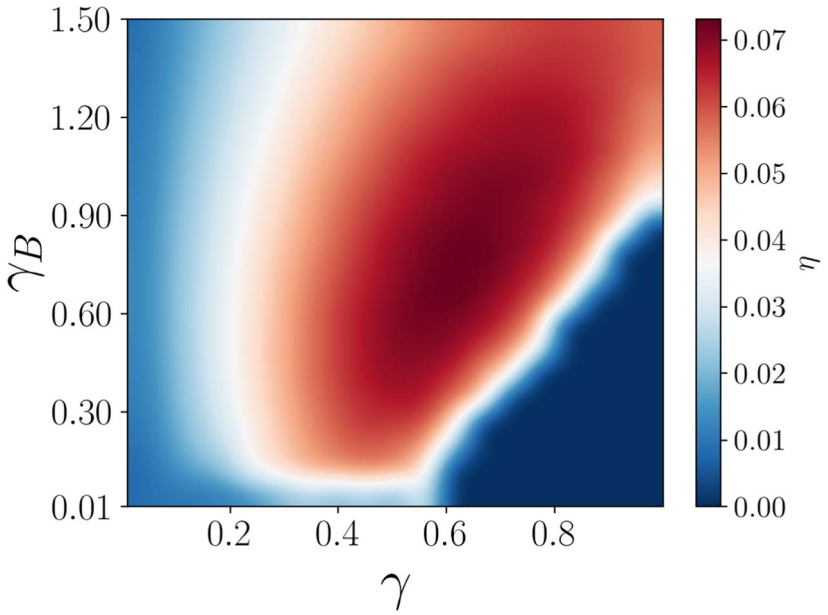

Figure 4. Phase diagram of the diode efficiency η as a function of the interface parameters $\gamma - \gamma_B$. The parameters of the calculation: $T = 0.1T_{cs}$, $d_s = 1.2\xi$, $d_f = \xi$, $H = 0.3$.

4. Discussion and conclusion

In summary we have examined the supercurrent diode efficiency in the TI based superconducting hybrid structure. Utilizing the microscopic formalism of the Usadel equations we have introduced a simple model of the S/F/TI structure to study the diode quality factor η as a function of various parameters of the structure. For this purpose we have examined the phase diagrams of η revealing the most favourable conditions for the SDE in the system. From $H - T$ diagram we have found that the highest diode quality factor is achieved at lower temperatures and at a specific H. From the same diagram we have recognized the critical field of the superconducting system. We have found the critical width d_s^{crit} on $d_s - d_f$ diagram that corresponds to the minimal d_s for the system to be in a superconducting state. Finally we have analyzed the diode quality factor as a function of the interface parameters. It has been shown that to reach the highest η it is optimal to have finite

transparency of the interface. These findings may help designing and developing the SDE devices based on the proximity effect.

Acknowledgments

The formulation of the model and the calculation of figure 2 were supported by Russian Science Foundation Project No. 23-72-30004. The calculation of figure 3 was supported by the Foundation for the Advancement of Theoretical Physics and Mathematics 'BASIS' grant number 22-1-5-105-1. The calculation of figure 4 was supported by the Mirror Laboratories Project and the Basic Research Program of the HSE University.

Data availability statement

All data that support the findings of this study are included within the article (and any supplementary files).

ORCID iDs

T Karabassov https://orcid.org/0000-0001-7966-5221
I V Bobkova https://orcid.org/0000-0003-1469-1861
A A Golubov https://orcid.org/0000-0001-5085-5195
A S Vasenko https://orcid.org/0000-0002-2978-8650

References

[1] Nadeem M, Fuhrer M S and Wang X 2023 The superconducting diode effect *Nature Reviews Physics* **5** 558–77
[2] Eschrig M 2015 *Rep. Prog. Phys.* **78** 104501
[3] Linder J and Robinson J W A 2015 *Nat. Phys.* **11** 307–15
[4] Daido A, Ikeda Y and Yanase Y 2022 *Phys. Rev. Lett.* **128** 037001
[5] He J J, Tanaka Y and Nagaosa N 2022 *New J. Phys.* **24** 053014
[6] Yuan N F Q and Fu L 2022 *PNAS* **119** e2119548119
[7] Scammell H D, Li J I A and Scheurer M S 2022 *2D Mater.* **9** 025027
[8] Ilić S and Bergeret F S 2022 *Phys. Rev. Lett.* **128** 177001
[9] Devizorova Z, Putilov A V, Chaykin I, Mironov S and Buzdin A I 2021 *Phys. Rev.* B **103** 064504
[10] de Picoli T, Blood Z, Lyanda-Geller Y and Väyrynen J I 2023 Superconducting diode effect in quasi-one-dimensional systems *Physical Review B* **107** 224518
[11] Grein R, Eschrig M, Metalidis G and Schön G 2009 *Phys. Rev. Lett.* **102** 227005
[12] Lu B, Ikegaya S, Burset P, Tanaka Y and Nagaosa N 2023 Tunable josephson diode effect on the surface of topological insulators *Physical Review Letters* **131** 096001 (arXiv: 2211.10572)
[13] Legg H F, Loss D and Klinovaja J 2022 *Phys. Rev.* B **106** 104501
[14] Ando F, Miyasaka Y, Li T, Ishizuka J, Arakawa T, Shiota Y, Moriyama T, Yanase Y and Ono T 2020 *Nature* **584** 373–6
[15] Bauriedl L, Bäuml C, Fuchs L, Baumgartner C, Paulik N, Bauer J M, Lin K, Lupton J M, Taniguchi T, Watanabe K, Strunk C, Paradiso N *et al* 2022 *Nature Communications* **13** 4266
[16] Shin J, Son S, Yun J, Park G, Zhang K, Shin Y J, Park J G and Kim D 2021 Magnetic proximity-induced superconducting diode effect and infinite magnetoresistance in a van der Waals heterostructure *Physical Review Research* **5** L022064
[17] Trahms M, Melischek L, Steiner J F, Mahendru B, Tamir I, Bogdanoff N, Peters O, Reecht G, Winkelmann C B, von Oppen F, Franke K J *et al* 2022 Diode effect in Josephson junctions with a single magnetic atom *Nature* **615** 628–33
[18] Chahid S, Teknowijoyo S, Mowgood I and Gulian A 2023 *Phys. Rev.* B **107** 054506
[19] Chahid S, Teknowijoyo S and Gulian A 2022 Quadristor: a novel device for superconducting electronics (arXiv: 2211.13340)
[20] Suri D, Kamra A, Meier T N G, Kronseder M, Belzig W, Back C H and Strunk C 2022 *Appl. Phys. Lett.* **121** 102601
[21] Hou Y, Nichele F, Chi H, Lodesani A, Wu Y, Ritter M F, Haxell D Z, Davydova M, Ilic S, Glezakou-Elbert O, Varambally A, Bergeret F S, Kamra A, Fu L, Lee P A, Moodera J S *et al* 2022 Ubiquitous superconducting diode effect in superconductor thin films *Phys Rev Lett* **131** 027001
[22] Narita H *et al* 2022 *Nat. Nanotechnol.* **17** 823–8
[23] Lyu Y, Jiang J, Wang Y, Xiao Z, Dong S, Chen Q, Milošević M V, Wang H, Divan R, Pearson J E, Wu P, Peeters F M and Kwok W 2021 Superconducting diode effect via conformal-mapped nanoholes *Nat Commun* **12** 2703
[24] Bocquillon E, Deacon R S, Wiedenmann J, Leubner P, Klapwijk T M, Brüne C, Ishibashi K, Buhmann H and Molenkamp L W 2017 *Nat. Nanotechnol.* **12** 137–43
[25] Baumgartner C *et al* 2022 *Nat. Nanotechnol.* **17** 39–44
[26] Wu H, Wang Y, Xu Y, Sivakumar P K, Pasco C, Filippozzi U, Parkin S S P, Zeng Y J, McQueen T and Ali M N 2022 *Nature* **604** 653–6
[27] Pal B *et al* 2022 *Nat. Phys.* **18** 1228–33
[28] Baumgartner C *et al* 2022 *J. Phys. Condens. Matter* **34** 154005
[29] Zhang Y, Gu Y, Li P, Hu J and Jiang K 2022 General Theory of Josephson Diodes *Physical Review X* **12** 041013
[30] Hu J, Wu C and Dai X 2007 *Phys. Rev. Lett.* **99** 067004
[31] Chen C Z, He J J, Ali M N, Lee G H, Fong K C and Law K T 2018 *Phys. Rev.* B **98** 075430
[32] Yokoyama T, Eto M and Nazarov Y V 2014 *Phys. Rev.* B **89** 195407
[33] Kopasov A A, Kutlin A G and Mel'nikov A S 2021 *Phys. Rev.* B **103** 144520
[34] Davydova M, Prembabu S and Fu L 2022 Universal Josephson diode effect *Science Advances* **8** eabo0309

[35] Halterman K, Alidoust M, Smith R and Starr S 2022 *Phys. Rev.* B **105** 104508
[36] Alidoust M, Shen C and Žutić I 2021 *Phys. Rev.* B **103** L060503
[37] Tanaka Y, Lu B and Nagaosa N 2022 Theory of giant diode effect in d-wave superconductor junctions on the surface of a topological insulator *Physical Review B* **106** 214524
[38] Golod T and Krasnov V M 2022 *Nat. Commun.* **13** 3658
[39] Kokkeler T, Golubov A and Bergeret F S 2022 Field-free anomalous junction and superconducting diode effect in spin-split superconductor/topological insulator junctions *Phys Rev B* **106** 214504
[40] Itahashi Y, Toshiya I, Yu S, Sunao S, Takumi O, Tsutomu N and Yoshihiro I 2020 *Sci. Adv.* **6** eaay9120
[41] Ryohei W, Yu S, Shintaro H M I Y, Toshiya I, Motohiko E, Yoshihiro I and Naoto N 2022 *Sci. Adv.* **3** e1602390
[42] Wakatsuki R and Nagaosa N 2018 *Phys. Rev. Lett.* **121** 026601
[43] Lin J X, Siriviboon P, Scammell H D, Liu S, Rhodes D, Watanabe K, Taniguchi T, Hone J, Scheurer M S and Li J I A 2022 *Nat. Phys.* **18** 1221–7
[44] Díez-Mérida J, Díez-Carlón A, Yang S Y, Xie Y, Gao X, Senior J, Watanabe K, Taniguchi T, Lu X, Higginbotham A P, Law K T, Efetov D K *et al* 2023 *Nat Commun* **14** 2396
[45] Edelstein V 1989 *Sov. Phys. JETP* **68** 1244
[46] Barzykin V and Gor'kov L P 2002 *Phys. Rev. Lett.* **89** 227002
[47] Dimitrova O and Feigel'man M V 2007 *Phys. Rev.* B **76** 014522
[48] Samokhin K V 2004 *Phys. Rev.* B **70** 104521
[49] Kaur R P, Agterberg D F and Sigrist M 2005 *Phys. Rev. Lett.* **94** 137002
[50] Houzet M and Meyer J S 2015 *Phys. Rev.* B **92** 014509
[51] Fulde P and Ferrell R A 1964 *Phys. Rev.* **135** A550–63
[52] Larkin A and Ovchinnikov Y 1965 *Sov. Phys. JETP* **20** 762
[53] Mironov S, Mel'nikov A and Buzdin A 2012 *Phys. Rev. Lett.* **109** 237002
[54] Mironov S V, Vodolazov D Y, Yerin Y, Samokhvalov A V, Mel'nikov A S and Buzdin A 2018 *Phys. Rev. Lett.* **121** 077002
[55] Bobkova I V, Bobkov A M, Zyuzin A A and Alidoust M 2016 *Phys. Rev.* B **94** 134506
[56] Karabassov T, Golubov A A, Silkin V M, Stolyarov V S and Vasenko A S 2021 *Phys. Rev.* B **103** 224508
[57] Karabassov T, Bobkova I V, Golubov A A and Vasenko A S 2022 *Phys. Rev.* B **106** 224509
[58] Burkov A A 2010 and Hawthorn D G *Phys. Rev. Lett.* **105** 066802
[59] Culcer D, Hwang E H, Stanescu T D and Das Sarma S 2010 *Phys. Rev.* B **82** 155457
[60] Yazyev O V, Moore J E and Louie S G 2010 *Phys. Rev. Lett.* **105** 266806
[61] Li C H, van 't Erve O M J, Robinson J T, Liu Y, Li L and Jonker B T 2014 *Nat. Nanotechnol.* **9** 218–24
[62] Zyuzin A, Alidoust M and Loss D 2016 *Phys. Rev.* B **93** 214502
[63] Bobkova I V and Bobkov A M 2017 *Phys. Rev.* B **96** 224505
[64] Kuprianov M Y and Lukichev V F 1988 *JETP Lett.* **67** 1163
[65] Bezuglyi E V, Vasenko A S, Shumeiko V S and Wendin G 2005 *Phys. Rev.* B **72** 014501
[66] Bezuglyi E V, Vasenko A S, Bratus E N, Shumeiko V S and Wendin G 2006 *Phys. Rev.* B **73** 220506
[67] Belzig W, Wilhelm F K, Bruder C, Schön G and Zaikin A D 1999 *Superlattices Microstruct* **25** 1251–88